J. Phys. D: Appl. Phys. **31** (1998) 2083–2090. Printed in the UK PII: S0022-3727(98)91426-7

The behaviour of ion-implanted tungsten species during anodic oxidation of aluminium

J C S Fernandes†, M G S Ferreira†, J C Soares‡, C M Jesus§, C M Rangel‖, P Skeldon¶, G E Thompson¶, X Zhou¶, H Habazaki+ and K Shimizu*

† Instituto Superior Tecnico, Grupo de Corrosão e Efeitos Ambientais, Avenida Rovisco Pais, 1096 Lisboa Codex, Portugal
‡ Instituto Tecnologico e Nuclear, Estrada Nacional 10, P-2685 Sacavém, Portugal
§ Centro de Fisica Nuclear, Universidade de Lisboa, Avenida Professore Gama Pinto 2, P-1699 Lisboa, Portugal
‖ Instituto Nacional de Engenharia e Technologia Industrial, Estrada do Paco do Lumiar, 1699 Lisboa Codex, Portugal
¶ Corrosion and Protection Centre, University of Manchester Institute of Science and Technology, PO Box 88, Manchester M60 1QD, UK
+ Institute for Materials Research, Tohoku University, 2-1-1 Katahira, Aoba-Ku, Sendai 980, Japan
* University Chemical Laboratory, Keio University, 4-1-1 Hiyoshi, Yokohama 223, Japan

Received 9 February 1998, in final form 18 May 1998

Abstract. Amorphous anodic oxide films have been formed at high efficiency on aluminium implanted with 3.0×10^{20} W ions m^{-2} in order to study the behaviour of tungsten during film growth. The initial film is composed mainly of alumina because the outer layer of aluminium above the main implanted region of the substrate is oxidized. During this period, tungsten atoms, present in low concentrations in the aluminium, accumulate in a thin metal layer just beneath the anodic film. Subsequently, the main tungsten-implanted region is oxidized, with incorporation of tungsten and aluminium species into the anodic film at the metal–film interface in proportion to their concentrations in the metal. The incorporated tungsten species migrate outwards in the anodic film at about 0.34 times the rate of Al^{3+} ions. After oxidation of the main tungsten-containing region, more dilute regions of metal containing about 1 at% W are consumed, with oxidation of aluminium and tungsten in the presence of a highly tungsten-enriched metal layer. The enrichment is initially equivalent to 15 ± 4 at% W, assuming that the enriched layer is 2 nm thick. However, later, as the metal–film interface reaches regions of metal containing about 0.1 at% W, the enriched layer contains significantly more tungsten than is usual for such dilute metal regions, indicating that tungsten is transported with the metal–film interface from metal regions of higher prior tungsten concentration as the film thickens.

1. Introduction

Ion implantation has been employed extensively for modifying the surface regions of materials, for alloys in particular to improve resistance to oxidation, corrosion and wear and to increase fatigue life [1]. Furthermore, ion implantation has facilitated studies of migration of species in anodic oxide films, through the use of implanted inert gas markers [2] and a relatively wide range of mobile implanted cations and anions [3]. Such studies have demonstrated that amorphous anodic films on high-purity metals are developed by migration of the metal cations and O^{2-} ions through the oxide film [4, 5]. Foreign species, introduced into the film by ion implantation or more naturally incorporated into the film at the metal–film interface, by formation of the film on an alloy substrate [6] or at the film–electrolyte interface, by transformation of electrolyte anions [7], generally migrate outwards or inwards, depending upon their charge.

The behaviour of certain ion-implanted species can be affected strongly by the preparation of the substrate prior to implantation [3]. Implantation directly into a pre-formed anodic oxide film usually results in uniform migration of the implanted species during subsequent thickening of the anodic film by re-anodizing [3]. In contrast, implantation into the metal can result in partial

incorporation of the implanted species into the film during subsequent anodizing, a significant fraction of the implanted dose remaining in the metal [3]. The elements that remain in the metal have oxidation potentials higher than that of aluminium [3].

Recent work on anodic oxidation of dilute aluminium alloys has also revealed that alloying elements associated with oxides of higher Gibbs free energy of formation per equivalent than that of alumina are retained within a roughly 2 nm thick alloy layer immediately beneath the anodic film until the alloy is sufficiently enriched for the oxidation of the alloying element to occur [8, 9]. Once oxidation of the alloying element begins, the enriched alloy layer retains an approximately constant amount of the alloying element during later film growth.

In the present study, the anodic oxidation of tungsten-implanted alloy is investigated in order to compare it with the behaviour of corresponding binary aluminium alloys. Tungsten was selected due to the existing knowledge of anodizing of Al–W alloys which, through the combination of transmission electron microscopy (TEM) and Rutherford backscattering spectroscopy (RBS), is readily examined [9, 10].

2. Experimental details

2.1. Specimen preparation

Specimens of high-purity (99.99%) aluminium, of dimensions 50 mm × 10 mm × 1 mm, were electropolished at 20 V in perchloric acid–ethanol (20:80 by volume) at 278 K. The specimens were then implanted with 3.0×10^{20} W ions m^{-2} at 150 keV, using the Danfysik 1090 High Current Implanter at the Instituto Tecnologico e Nuclear (ITN), Sacavém.

The retained dose, measured by RBS after implantation, was $(3.0 \pm 0.1) \times 10^{20}$ W atoms m^{-2}, indicating that sputtering during implantation was negligible. The depth of the maximum concentration of tungsten and the FWHM of the tungsten distribution, determined by the TRIM code, were 55 and 30 nm respectively. The estimated maximum concentration of tungsten was about 16 at%. The specimens were then anodized at 50 A m^{-2} to 100, 150 or 280 V in aqueous 0.1 M ammonium pentaborate electrolyte at 293 K. Anodic films are formed on Al–W alloys at approximately 100% efficiency in this electrolyte [9, 10]. A two-electrode cell, containing 200 ml of stirred electrolyte and a cylindrical aluminium cathode, was employed for anodizing, with the current supplied by a Metronix 6912 constant current power source. The current was switched off immediately the selected voltage had been reached. The voltage–time response during anodizing was recorded on a chart recorder.

2.2. Examination of specimens

Sections about 10 nm thick at right angles to the specimen's surface both of as-implanted and of anodized specimens were prepared by ultramicrotomy for examination in a JEOL FX 2000 II transmission electron microscope equipped with energy dispersive x-ray (EDX) analysis facilities. The compositions of specimens were determined by RBS using a 1.6 MeV beam of α particles supplied by the 3.1 Van de Graaff accelerator of ITN, Sacavém. The α particles were detected at 180° using an annular silicon surface barrier detector with resolution 18 keV. The specimen was rotated by 50° to enhance depth resolution. The data were analysed by the RUMP program [11], with scaling of the stopping power of oxygen by 0.88 [12].

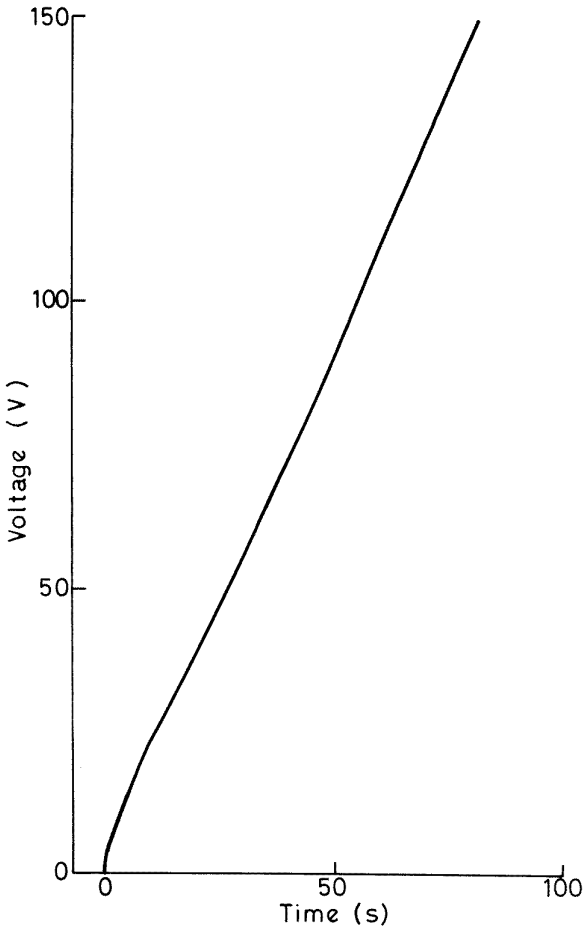

Figure 1. The voltage–time response for anodizing electropolished aluminium, implanted with tungsten to a dose of 3.0×10^{20} W atoms m^{-2}, at 50 A m^{-2} in 0.1 M ammonium pentaborate electrolyte at 293 K.

3. Results

3.1. The voltage–time response

The voltage–time response revealed reproducible features, comprising a voltage surge due to the initial air-formed film at a specimen's surface, a linear region to about 19 V of slope about 2.3 V s^{-1} and an inflection leading to a region of initial slope about 1.8 V s^{-1} at about 30 V, in which the slope gradually increases with anodizing, approaching about 2.1 V s^{-1} at the highest voltage (figure 1). The slope following the initial voltage surge is similar to that for anodizing high-purity aluminium. A reduction in slope

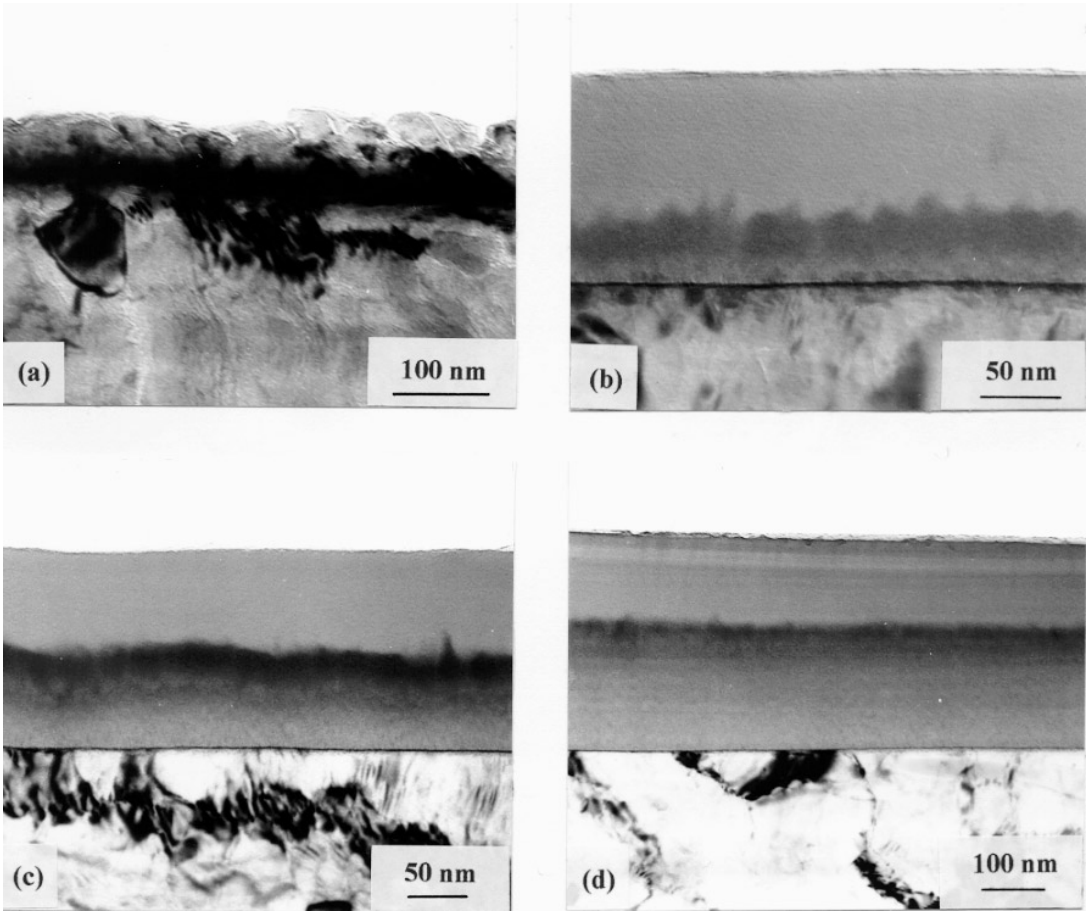

Figure 2. Transmission electron micrographs of ultramicrotomed sections of electropolished aluminium implanted with tungsten to a dose of 3.0×10^{20} W atoms m^{-2}: (a) as implanted, (b), (c) and (d) anodized at 50 A m^{-2} to 100, 150 and 280 V respectively in 0.1 M ammonium pentaborate electrolyte at 293 K.

is anticipated with incorporation of tungsten species into the film [10].

3.2. Transmission electron microscopy

The section of the as-implanted specimen reveals a continuous dark layer, about 40 nm thick and located about 40 nm beneath the specimen surface, due to the high concentration of tungsten atoms in this region (figure 2(a)). The depth of the mid-thickness of the layer, about 60 nm, is in good agreement with the depth of the maximum concentration of tungsten estimated using the TRIM code, about 55 nm. Similarly the thickness of the layer, about 40 nm, is consistent with the estimated FWHM of 30 nm. Precise agreement with TRIM results is not expected due to effects of the ion beam on the material and the qualitative assessment of the tungsten distribution by TEM. The overlying lighter layer, appearing similar to the bulk aluminium, evidently contains less tungsten; this layer appears to have been damaged during implantation, with the development of a rough surface and fine cracks. The distortion of the substrate apparently extends about 40 nm beneath the main implanted region, although the distortion at greater depth may be due to sectioning.

Following anodizing to 100 V, an amorphous anodic film of thickness 127 ± 4 nm is formed, the main part of which is similar in appearance to anodic alumina (figure 2(b)). The thickness-to-voltage ratio of 1.27 nm V^{-1} compares with about 1.2 nm V^{-1} for anodizing of high-purity aluminium [13]. A slightly higher value is anticipated for the ion-implanted material because the resistivity of tungsten-contaminated alumina is lower. The innermost $36 \pm 3\%$ of the film's thickness is darker than the remainder of the film due to incorporation of units of WO_3 into the alumina structure through anodic oxidation of the main tungsten-containing region of the implanted substrate. The aluminium is enriched in tungsten, compared with underlying metal, in a layer about 2 nm thick just beneath the anodic film. The metal within about 20 nm of the enriched layer is occasionally darker than the main bulk of the aluminium, possibly owing to corrosion of the enriched layer during ultramicrotomy with relocation of dissolved tungsten species at cathodic sites in surrounding regions of metal.

The film's thickness increases to 169 ± 3 nm upon anodizing to 150 V, with tungsten species occupying the innermost $50 \pm 3\%$ of the film's thickness (figure 2(c)). The thickness-to-voltage ratio, namely 1.13 nm V^{-1}, is similar to that for growth of anodic alumina, which is reasonable insofar as later RBS analysis reveals that tungsten species represent only about 5% of the cations in the film. The

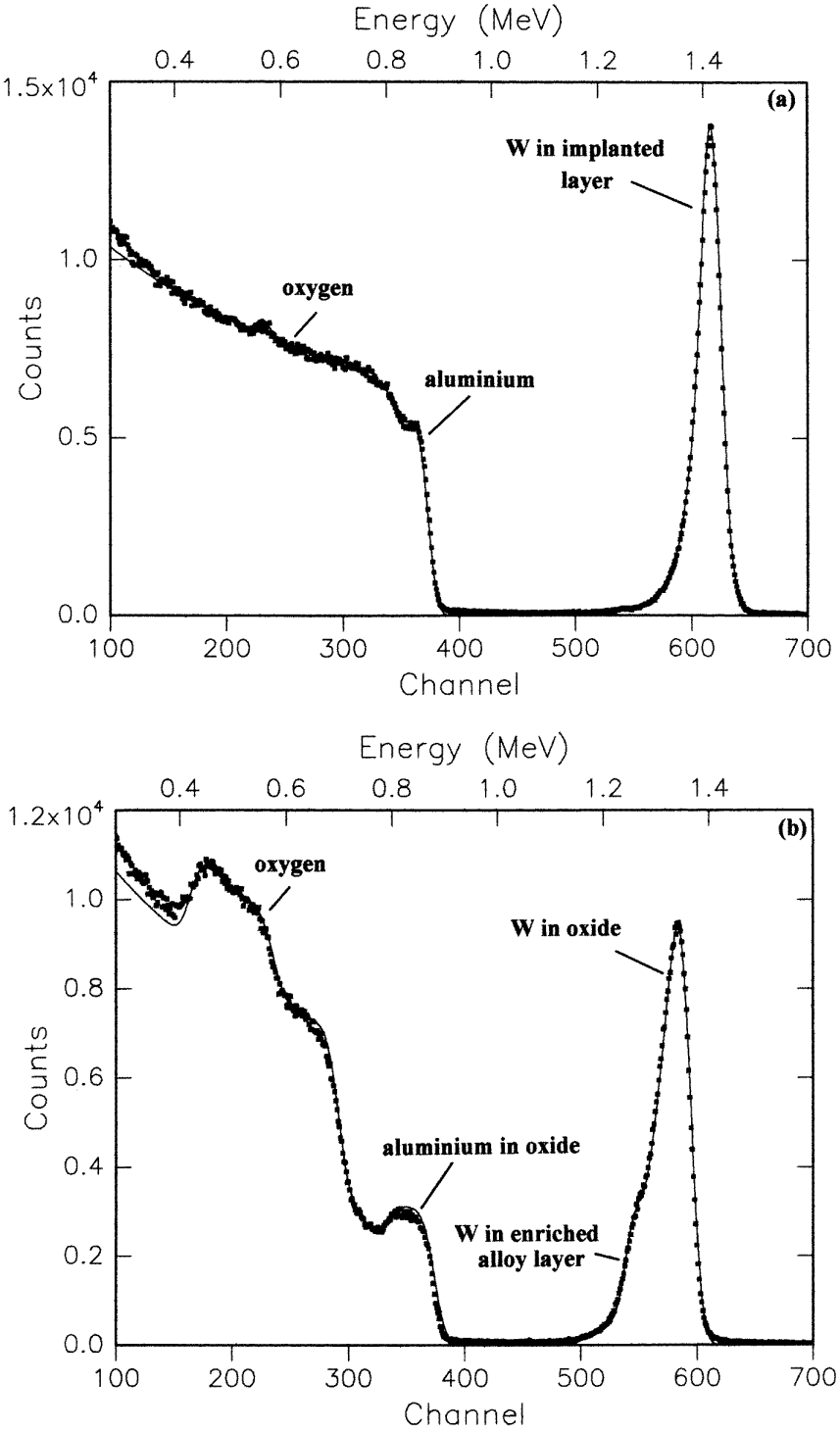

Figure 3. Experimental and simulated (line) RBS spectra for electropolished aluminium implanted with tungsten to a dose of 3.0×10^{20} W atoms m^{-2}: (a) as implanted, (b) anodized at 50 A m^{-2} to 150 V in 0.1 M ammonium pentaborate electrolyte at 293 K and (c) the distribution of tungsten in the anodic film from (b) (table 1). M/F denotes the metal–film interface.

main tungsten-containing region appears darker than that in the previous micrograph which is an effect of the section's thickness. The whole of the innermost region evidently contains tungsten species, though the graded contrast suggests that the tungsten concentration decreases towards the metal–film interface. The tungsten-enriched metal layer adjacent to the metal–film interface is similar to that of the previous specimen.

With anodizing to 280 V the film's thickness increases to 338 ± 8 nm, corresponding to a ratio of 1.21 nm V^{-1}, and tungsten species are confined to the innermost $61 \pm 3\%$ of the film's thickness (figure 2(d)). A tungsten-enriched

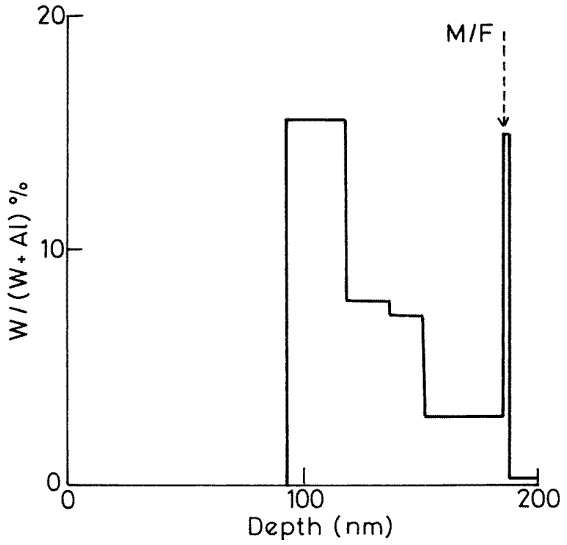

(c)

Figure 3. (Continued)

metal layer is disclosed adjacent to the metal–film interface; the film material immediately above the interface reveals no direct evidence of the presence of tungsten species.

3.3. Rutherford backscattering spectroscopy

The RBS spectra for the as-implanted specimen reveal the expected yields from tungsten and aluminium nuclei (figure 3(a)). The main amount of tungsten is buried about 42 nm beneath the aluminium surface and is contained within a layer about 37 nm thick. The maximum concentration of tungsten in the simulated profile, namely 9.4 at% in a 36.5 nm thick layer (table 1), is reasonably consistent with the maximum of about 16 at%, in a thinner layer, from TRIM calculations. The tungsten concentration decreases at greater depths, reaching about 1 at% at about 125 nm. The outer 27 nm of the specimen was assumed to contain oxygen in order to fit the small oxygen peak located upon the yield from aluminium. The oxygen, equivalent to that in a roughly 6 nm thick alumina film, probably arises from redistribution of the oxygen of the air-formed alumina film during implantation and re-formation of the film after implantation.

Following anodizing to 150 V, the tungsten yield shifts to lower energies due to the formation of an outer alumina-rich layer, 93 nm thick (table 1, figure 3(c)), above the main tungsten-containing region of film material (figure 3(b)). Beneath the region of film of high tungsten concentration, corresponding to about 16 at% W considering cations only, the concentration decreases to about 3 at% W near the metal–film interface. The particular simulation was performed in order to obtain the best fit to the regions corresponding to scattering from aluminium and tungsten nuclei near the metal–film interface, which required the use of an artificially high detector resolution of 40 keV. This high resolution was necessary in order to simulate the apparent non-uniformity of the film's thickness, which is possibly due to a lack of flatness of the substrate over the area of analysis. This manipulation results in overestimation of the maximum concentration of tungsten in the main tungsten-containing layer. Using a more realistic detector resolution of 18 keV, the concentration of tungsten in the main tungsten-containing layer of film material is about 13 at% W in a roughly 22 nm thick layer of film material. The thickness of the inner, tungsten-containing region is about 51% of the total film thickness in agreement with the result from TEM. The total amount of tungsten in the film, namely $(2.8 \pm 0.1) \times 10^{20}$ W atoms m^{-2}, indicates that no significant loss of tungsten occurred during anodizing.

The yield from tungsten reveals a shoulder on the lower energy side of the peak which is associated with the tungsten-rich metal layer adjacent to the metal–film interface. The amount of tungsten in the enriched layer is estimated to be 15 ± 4 at%, assuming that the layer is 2 nm thick (table 1), equivalent to $(1.7 \pm 0.4) \times 10^{19}$ W atoms m^{-2}.

4. Discussion

4.1. Anodizing of aluminium and aluminium alloys

Prior to considering the present results, anodizing of aluminium and aluminium alloys is briefly reviewed to assist interpretation of data. The growth of anodic alumina films on aluminium proceeds by migration of Al^{3+} and O^{2-} ions through the alumina with transport numbers of about 0.4 and 0.6 respectively [2]. Anodizing of dilute aluminium alloys is similar to that of aluminium, although alloying element species are incorporated into the film from the substrate. The incorporation of such species may be delayed until the alloy region immediately beneath the film is sufficiently enriched in the alloying element by the initial growth of an essentially alumina film [9]. For more concentrated alloys, the period of enrichment is either nonexistent or negligible [14]. The presence of alloying element species in the anodic film leads to changes in the transport numbers of migrating ions and also in the relative migration rates of the alloying element cations and Al^{3+} ions [14]. However, the changes in transport numbers for Al–W alloys are probably small due to the similarity of the transport numbers for anodic alumina and anodic WO_3 [15].

4.2. Anodizing of tungsten-implanted aluminium

The present results reveal features of anodizing of ion-implanted aluminium originally reported by Mackintosh *et al* [3]. However, they did not include tungsten or consider the mechanism of incorporation of implanted species into anodic films, which is now shown to be understandable in terms of the anodizing mechanism of Al–W alloys [9].

For incorporation of cation species into an anodic alumina film at the metal–film interface, the ratio, r, of

Table 1. Results of simulations (shown in figure 3) of RBS data of electropolished aluminium implanted with tungsten to a dose of 3.0×10^{20} W atoms m^{-2}, both as-implanted and following anodizing at 50 A m^{-2} to 150 V in 0.1 M ammonium pentaborate electrolyte at 293 K. The layers are listed in order starting from the surface of the specimen. The ionic density of anodic film material is assumed to be the same as that of usual anodic alumina, namely 0.915×10^{29} m^{-3}.

	As implanted		Anodized to 150 V	
Layer	Composition (at% W)	Thickness (nm)	Composition (at% W)	Thickness (nm)
1	$AlO_3W_{0.008}$	26.8	Al_2O_3	93
2	0.88	15.2	$Al_2O_3 \cdot 0.370WO_3$	25
3	9.40	36.5	$Al_2O_3 \cdot 0.172WO_3$	18
4	2.60	30.4	$Al_2O_3 \cdot 0.155WO_3$	15
5	1.37	15.2	$Al_2O_3 \cdot 0.059WO_3$	34
6	0.72	15.2	15.2	2
7	0.47	15.2	0.22	35
8	0.37	15.2	0.20	35
9	0.28	15.2	0.11	30
10	0.11	15.2	0	5000
11	0.10	30.4		
12	0.08	30.4		
13	0	5000		

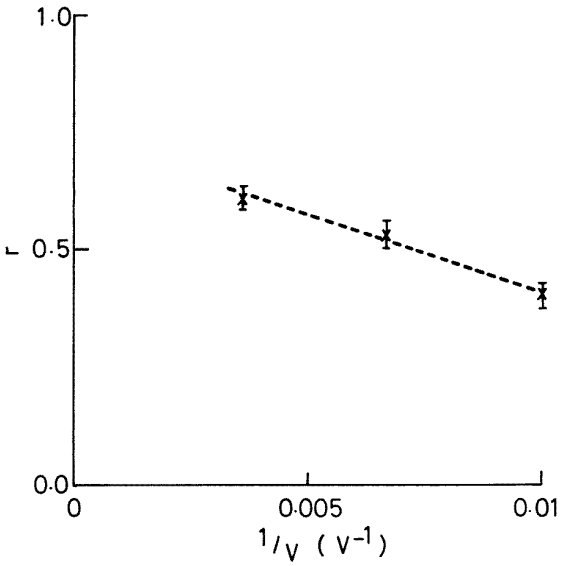

Figure 4. The ratio of the thickness of the tungsten-containing region of film material to the total film thickness (r) versus the inverse of the anodizing voltage for anodizing electropolished aluminium, implanted with tungsten to a dose of 3.0×10^{20} W atoms m^{-2}, at 50 A m^{-2} in 0.1 M ammonium pentaborate electrolyte at 293 K.

the maximum distance of the incorporated species from the interface to the total film thickness is given by

$$r = (0.6 + 0.4u_0)[1 - (V_0/V)]$$

in which u_0 is the migration rate of the incorporated species relative to that of Al^{3+} ions, V_0 is the anodizing voltage at which the species are first incorporated into the film and V is the final anodizing voltage [9]. The results for the present films indicate that the tungsten species migrate outwards at 0.34 ± 0.03 times the rate at which Al^{3+} ions migrate, with a V_0 value of 45 ± 4 V (figure 4). Here the low concentration of tungsten in the outer aluminium layer above the main region of implantation has been neglected. The migration rate is in satisfactory agreement with rates of about 0.38 determined from study of anodized Al–W alloys [9, 17]. The delay in incorporation of tungsten species is explained by considering the depth of implantation of the main dose, namely about 40 nm, from TEM, beneath the specimen's surface. Furthermore, some short period of accumulation of tungsten in the metal-enriched layer as the retreating metal–film interface enters the region of higher tungsten concentration may be necessary in order to establish the level of enrichment for oxidation of tungsten to proceed, though the main amount is probably achieved when the outer dilute implanted layer is oxidized. Assuming a ratio 1.2 nm V^{-1} and a Pilling–Bedworth ratio of 1.65, namely that for formation of alumina of density 3.1 Mg m^{-3} [14], about 33 nm of metal is oxidized prior to incorporation of tungsten species into the anodic film, which is in satisfactory agreement with the thickness of material above the main implanted layer indicated by TEM. The estimated voltage at which tungsten species are incorporated into the film is higher than the inflection voltage in the voltage–time response, which may indicate that the latter is associated with oxidation of a more damaged, higher resistivity, outer layer of the as-implanted material, containing a significant amount of oxygen.

The RBS simulation indicates that there is an average concentration of about 9 at% W in the main implanted region, the peak concentration probably approaching the calculated value of about 16 at% W. For such concentrations of tungsten in bulk alloys, incorporation of tungsten species into the anodic film proceeds following anodic oxidation of about 1 nm of alloy. Owing to the slower migration of tungsten species in the anodic film, relative to that of Al^{3+} ions, the concentration of tungsten species in the film is enhanced relative to that in the substrate. The expected average concentration of tungsten in the main tungsten-containing layer of film material, based on the measured concentration in the main tungsten-containing layer of the as-implanted specimen and the determined migration rate, is about 12 at% W [9], in satisfactory agreement with the RBS result. Locally

higher concentrations are probably present, for the TRIM code indicates that there is a maximum concentration of about 16 at% W in the as-implanted alloy. However, ionic mixing during film growth will reduce the maximum concentration in the film to less than that estimated from simple theory [18]. Furthermore, peak concentrations are not resolved by RBS due to the limitation of its depth resolution. Following the oxidation of the main implanted region, the metal–film interface enters a region of metal of much lower tungsten content, <3 at% at a depth of about 80 nm from the original metal surface. This thickness of metal is consumed during anodizing to about 110 V. Anodic oxidation then proceeds similarly to that of a dilute Al–W alloy, tungsten and aluminium being oxidized at the metal–film interface in the immediately underlying alloy proportions. The oxidation of the tungsten occurs locally, resulting in fingers of tungsten-rich oxide originating at the metal–film interface [9]. The local oxidation has been attributed to the presence of tungsten-rich clusters in the enriched alloy layer [9], which move inwards relative to the original metal surface, carried by the retreating alloy–film interface. Previous work has revealed similar transport of xenon, which has been suggested to be present as fine bubbles at the metal–film interface [19]. There is probably an adjustment of the enrichment of tungsten as the metal–film interface moves into regions of metal containing less tungsten. However, previous work suggests that the enrichment is relatively high, namely about 20 at% W in a 2 nm thick layer, down to alloy concentrations of about 1 at% W [17]. The ultramicrotomed section of the anodic film formed to 150 V shows the typical features of an anodized sputter-deposited Al–W alloy containing about 1 at% W. Following anodizing to 150 V, about 109 nm of alloy is consumed, RBS indicating that the metal contains about 1–2 at% W at this depth.

As anodizing progresses, the metal–film interface enters more dilute metal regions: at 280 V, about 204 nm of metal has been consumed and the tungsten concentration is about 0.1 at%. Previous work on an alloy of this concentration has shown that oxidation of tungsten and aluminium species proceeds in the presence of an enrichment of about 2.5 at% W in an assumed 2 nm thick alloy layer [17]. The enrichment is too low to be visible in TEM micrographs. In contrast, the enriched metal layer is readily discerned for the tungsten-implanted specimen anodized to 280 V. Clearly the enriched layer has retained a tungsten concentration characteristic of the metal regions of higher prior tungsten content.

The consequences of the enrichment of tungsten for the corrosion resistance of the anodized surfaces have not been investigated, but related work on the influence of enrichment in tungsten beneath the passive film formed on non-equilibrium Al–W alloys has indicated that it has beneficial effects, by greatly increasing resistance to pitting over a wide range of pH [20]. An enhancement of passivity has also been reported for Al–Ta alloys, which develop enrichments of tantalum [21]. The tungsten and tantalum enrichments are considered to inhibit pit nucleation and assist repassivation due to the stability of the alloying elements' oxides in acidic environments. Similar benefit may be anticipated for the anodized ion-implanted specimens, with a dependence upon the thickness of anodic film which affects the level of enrichment of tungsten.

5. Conclusions

(i) The anodic oxidation of aluminium implanted with about 3×10^{20} W atoms m^{-2} in ammonium pentaborate electrolyte is consistent with the anodizing behaviour of binary Al–W alloys. The initial oxidation proceeds with formation of a mainly alumina film containing relatively little tungsten as the outer aluminium region above the main implanted region is oxidized. During this stage, there is some accumulation of tungsten, which is present in relatively low concentration in the outer aluminium layer, in a thin metal layer adjacent to the metal–film interface.

(ii) Following oxidation of the outer mainly aluminium metal layer, the main tungsten-implanted region, containing an average concentration of about 9 at% W, is oxidized with incorporation of aluminium and tungsten species into the anodic film. The tungsten species migrate outwards in the anodic film at about 0.34 the rate at which Al^{3+} ions migrate, which is similar to the rate of migration of tungsten species in anodic films formed on Al–W alloys.

(iii) Subsequently, the oxidation of the underlying implanted regions of lesser tungsten concentration takes place, with incorporation of tungsten and aluminium species into the film in the presence of a tungsten-enriched metal layer containing about 15 at% W assuming a layer of 2 nm thickness. The degree of enrichment is initially similar to that expected during anodizing of a dilute Al–W alloy of composition equal to that of the implanted metal immediately beneath the anodic film. However, the enrichment of the metal is later enhanced greatly relative to the expected value for the appropriate dilute Al–W alloy, indicating that tungsten in the enriched metal layer is transported inwards into the metal substrate.

Acknowledgment

The authors are grateful to M F da Silva (ITN) for assistance with RBS measurements.

References

[1] Smith F A (ed) 1983 *Ion Implantation for Materials Processing* (New Jersey: Noyes Data Corporation)
[2] Brown F and Mackintosh W D 1973 *J. Electrochem. Soc.* **120** 1096
[3] Mackintosh W D, Brown F and Plattner H H 1974 *J. Electrochem. Soc.* **121** 1281
[4] Pringle J P S 1973 *J. Electrochem. Soc.* **120** 398
[5] Pringle J P S 1980 *Electrochim. Acta* **25** 1423
[6] Ruth R L and Schwartz N 1976 *J. Electrochem. Soc.* **123** 1869
[7] Konno H, Kobayashi S, Takahashi H and Nagayama M 1980 *Electrochim. Acta* **25** 1667
[8] Habazaki H, Shimizu K, Skeldon P, Thompson G E, Wood G C and Zhou X 1997 *Trans. Inst. Met. Finishing* **75** 18
[9] Habazaki H, Shimizu K, Skeldon P, Thompson G E and Wood G C 1996 *Phil. Mag.* B **73** 445
[10] Habazaki H, Shimizu K, Skeldon P, Thompson G E and Wood G C 1994 *Phil. Mag.* B **71** 81

[11] Doolittle L R 1985 *Nucl. Instrum. Methods* B **9** 344
[12] Cheang Wong J C, Li J, Ortega C, Siejka J, Vizkelethly G and Lemaitre Y 1992 *Nucl. Instrum. Methods* B **64** 169
[13] Harkness A C and Young L 1966 *Can. J. Chem.* B **44** 2409
[14] Habazaki H, Shimizu K, Skeldon P, Thompson G E and Wood G C 1997 *Proc. R. Soc.* A **453** 1593
[15] Davies J A, Domeij B, Pringle J P S and Brown F 1965 *J. Electrochem. Soc.* **112** 765
[16] Skeldon P, Shimizu K, Thompson G E and Wood G C 1983 *Surf. Interface Anal.* **5** 247
[17] Habazaki H, Shimizu K, Skeldon P, Thompson G E and Wood G C 1996 *J. Electrochem. Soc.* **143** 2465
[18] Habazaki H, Skeldon P, Thompson G E, Wood G C and Shimizu K 1996 *Phil. Mag.* B **73** 297
[19] Thomas J P, Fallavier M, Spender P and Francois E 1980 *J. Electrochem. Soc.* **127** 585
[20] Davis G D, Shaw B A, Rees B J and Ferry M 1993 *J. Electrochem. Soc.* **140** 951
[21] Davis G D, Shaw B A, Rees B J and Pecile C A 1995 *Surf. Interface Anal.* **23** 609